

OBSERVATION ON A FIRE WHIRL IN A VERTICAL SHAFT USING HIGH-SPEED CAMERA AND ASSOCIATED CORRELATION DERIVED

by

**Hing Yeung HUNG^a, Shousuo HAN^a, Wan Ki CHOW^{a*},
and Cheuk Lun CHOW^b**

^aResearch Centre for Fire Engineering, Department of Building Services Engineering,
Hong Kong Polytechnic University, Hong Kong, China

^bDepartment of Architecture and Civil Engineering, City University of Hong Kong,
Hong Kong, China

Original scientific paper
<https://doi.org/10.2298/TSCI181004266H>

The fire whirl generated by burning a pool fire in a vertical shaft with a single corner gap of appropriate width was studied using a high-speed camera. A 7 cm diameter pool propanol fire with heat release rate 1.6 kW in free space was burnt inside a 145 cm tall vertical shaft model with gap widths lying between 2 cm and 16 cm. The flame height was between 0.25 m and 0.85 m for different gap widths. Photographs taken using a high-speed camera at critical times of swirling motion development were used to compare with those taken using a normal camera. From the experimental observations on flame swirling by a high-speed camera, stages for generating the fire whirl were identified much more accurately. Two flame vortex tubes moving over the horizontal burning surface of the liquid pool were observed. Based on these observations a set of more detailed schematic diagrams on the swirling motion was constructed. From the observed flame heights under different gap widths and using three assumptions on the variation of air entrainment velocity with height, an empirical expression relating the burning rate with flame height and the corner gap width was derived from the observation with high-speed camera. The correlation expression of the burning rate of the pool fire obtained would be useful in fire safety design in vertical shafts of tall buildings.

Key words: *internal fire whirl, vertical shaft, corner gap width, burning rate*

Introduction

Different arrangements for generating a fire whirl inside an enclosure were reported in the literature [1-10]. The fire whirl is called an internal fire whirl (IFW) in this study to distinguish it from the external fire whirl which might move over the burning fuel. An IFW has a fixed physical fire size, and does not spread over the fuel surface as in open space. An IFW can be created in a vertical shaft in tall buildings with appropriate sidewall ventilation arrangement [11-15]. This is hazardous to green buildings with tall shafts or good thermal insulation [16-18] and studied as a long-term project. As reviewed on fire whirls [19], the flame height was extended several times longer with the burning rate significantly increased. Correlations of the flame height of IFW with the vortex parameters were investigated [10] through theoretical analysis, experiments and numerical simulations.

* Corresponding author, e-mail: elize.yeung.polyu@gmail.com; bewkchow@polyu.edu.hk

In a vertical shaft with a corner gap, the gap width affects the ventilation and hence the air supply rate to the fire, which changes the burning rate. Once the burning rate is changed, the hydrodynamics induced by the fire is also changed, giving swirling flame characteristics. A correlation expression of the IFW flame height in a 9 m tall vertical shaft with corner gap width has been reported recently [20].

Swirling flame patterns were observed using a high-speed camera in this long-term research project [11-15] and reported in this paper. Flame heights measured were compared with those observed from a normal camera. As a high-speed camera can provide more details in the development of swirling flame patterns, it is possible to identify different stages of IFW development more accurately. An expression correlating the burning rate of the pool fire with the corner gap width in an IFW can be derived based on small model experiments. Earlier results [*e. g.* 19] can then be justified.

Experimental studies

A fire whirl can be generated by burning a pool fire in a vertical shaft model of appropriate gap widths [11-15, 20]. Such experiments were carried out to investigate the effect of the gap width on IFW generation.

The vertical shaft model used was of section 35 cm by 34 cm (with the gap) and height 145 cm, as shown in fig. 1(a). The model was made of wood with a transparent plastics sheet for observing the flame shape and taking pictures. Experiments on varying the width of the vertical gap were carried out with some results reported previously [11, 13-15].

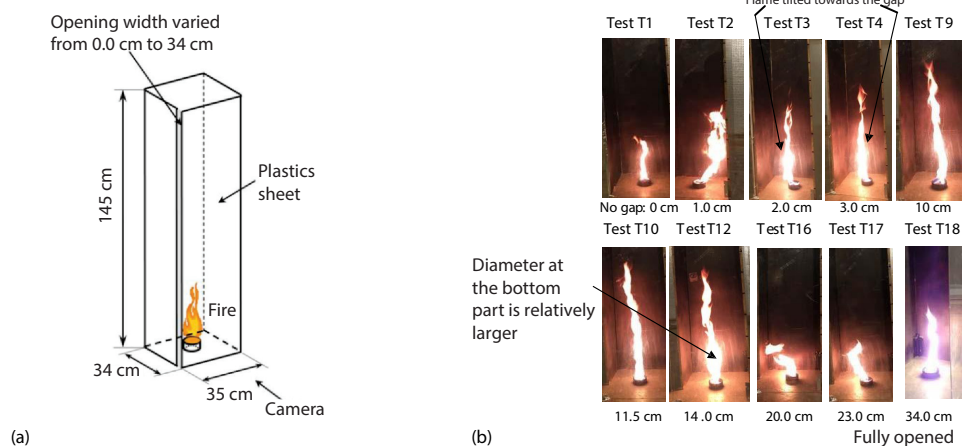


Figure 1. Tests on a vertical shaft model; (a) the vertical shaft model, (b) flame height taken using a normal camera

A 1.6 kW pool fire of diameter, D , of 7 cm and containing 25 ml propanol was placed on the ground at the centre of the shaft model. The burning time, t_B [s], for the same pool fire in outside air was about 400 seconds. The average heat release rate was 1.6 kW with maximum flame height of 40 cm and average flame height of 20 cm while burning the pool fire outside.

There were 18 tests labeled T1-T18 with different gap widths d_g [cm] of values 0.0 cm (gap closed), 1.0 cm, 2.0 cm, 3.0 cm, 4.0 cm, 4.3 cm, 6.8 cm, 8.5 cm, 10.0 cm, 11.5 cm, 12.8 cm, 14 cm, 16 cm, 17 cm, 18.4 cm, 20 cm, 23 cm, and 34 cm (gap fully opened, that is, with one

Table 1. Results for the tests with different gap width

Test No.	Vertical gap width, d_g [cm]	Vertical gap width ratio, d_g/a [cm]	Burning time, t_b [s]	Fire whirl generated, Y/N	Stable IFW, Y/N	Fire whirl start time [s]	Fire whirl duration [s]	Maximum flame height, f_{max} [cm]	Average flame height, f_h [cm]	Average mass loss rate over t_b , m_{av1} [gs^{-1}]	Average mass loss rate over fire whirl, m_{av2} [gs^{-1}]	Average mass loss rate by measuring transient mass, m_{av3} [gs^{-1}]
T1	0.0	0	380	N	N	–	0	40	20	0	–	–
T2	1.0	0.03	252	NA	N	–	NA	50	25	0.029	–	–
T3	2.0	0.06	150	Y	Y	15	130	80	55	0.131	0.151	0.124
T4	3.0	0.09	144	Y	Y	9	130	85	65	0.136	0.151	0.125
T5	4.0	0.12	150	Y	Y	6	140	85	65	0.131	0.140	0.136
T6	4.3	0.13	150	Y	Y	8	140	85	65	0.131	0.140	0.133
T7	6.8	0.20	155	Y	Y	6	145	80	60	0.127	0.135	0.121
T8	8.5	0.25	180	Y	Y	6	160	75	55	0.109	0.123	0.114
T9	10	0.29	180	Y	Y	7	160	70	55	0.109	0.123	0.098
T10	11.5	0.33	180	Y	Y	5	160	65	50	0.109	0.123	0.096
T11	12.8	0.38	180	Y	Y	5	160	65	45	0.109	0.123	0.070
T12	14	0.42	180	Y	Y	6	160	60	40	0.109	0.123	0.069
T13	16	0.46	180	Y	Y	6	160	60	40	0.109	0.123	0.061
T14	17	0.50	250	NA	N	–	NA	55	30	0.079	–	–
T15	18.4	0.54	300	NA	N	–	NA	50	25	0.065	–	–
T16	20	0.58	360	N	N	–	0	45	22	0.055	–	–
T17	23	0.67	395	N	N	–	0	40	20	0.050	–	–
T18	34	1	400	N	N	–	0	40	20	0.049	–	–

* NA indicates there might be unstable fire whirl with short duration

wall was removed), respectively. The ratio d_g/a of gap width d_g to wall width a (of 34 cm) lies between 0 and 1. A summary of the 18 tests is shown in tab. 1.

The burning time of the propanol pool fire varied from 144-400 seconds, depending of gap width.

Observations using normal camera

Videos and photographs were taken using a normal digital camera through the transparent surface for each test to determine the flame lengths of the propanol pool fire in the vertical shaft under different corner gap widths.

The flame shapes during steady burning for some of the 18 tests are shown in fig. 1(b). For pool fire in the shaft model with no corner gap, flame did not swirl. The flame behaved in a manner similar to that of a pool fire in free space.

In the case of 1 cm gap opening, the amount of air that could be entrained into the shaft was relatively small and no IFW was formed. However, the flame revolved in counter-clockwise direction as shown in photographs and video captured using a normal camera, fig. 2.

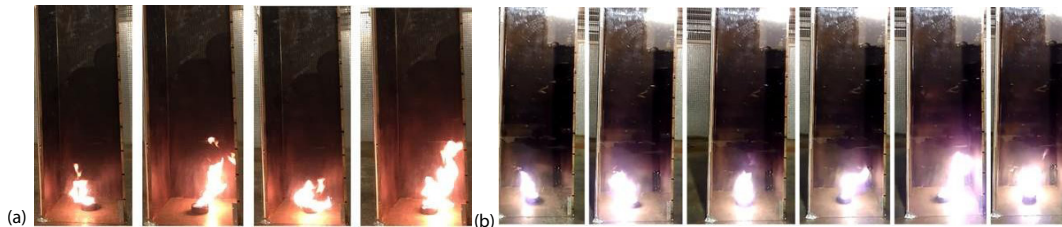


Figure 2. Flame revolved in counterclockwise direction for test T2 with 1 cm gap width; (a) captured from a normal camera, (b) captured from video

As the gap width increased to 2 cm and 3 cm in tests T3 and T4, an IFW was formed. In addition, the flame tilted slightly towards the gap opening as shown in fig. 1(b).

Regarding the cases with gap width of 4-10 cm, an IFW was also formed. The IFW was much stable as the flame kept rotating about the central axis and did not appear to tilt to other directions.

Compared to the IFW formed in the cases with gap width of 4-10 cm, the IFW formed in the cases with gap width of 11.5-16 cm was slightly less stable as it again tilted towards the gap opening. Moreover, the flame diameter at the lower part of the IFW was slightly larger as shown in fig. 1(b).

The flame tilted towards the gap for d_g of 2-3 cm in tests T3 and T4 because the IFW was not stable enough and so affected by incoming air movement from the gap. The larger flame diameter at the lower part of the IFW for tests with larger gap width because it allowed more air to enter the shaft model to support more vigorous combustion.

There are three types of flame characteristics observed for the different gap widths:

- No fire whirl was observed and flames moved round occasionally about a vertical axis for the tests with an opening width over 19 cm or less than 1 cm.
- Swirling motions were observed for a short time or unstable fire whirls were created for the tests with an opening width from 1 cm to 2 cm, and from 16 cm to 19 cm.
- Stable IFW were observed for the tests with an opening width from 2-16 cm, or d_g/a ratio from 1/17 to 8/17.

When the corner gap width increased beyond 16 cm, both flame rotation and precession were weakened. The pool fire behaved as that in free space again when the gap width was bigger than 19 cm.

For gap width half the width of the shaft model (that is, width of 17 cm or d_g/a of 0.5), more air was entrained into the shaft model. This would disturb the stable IFW motion. Therefore, 17 cm is a critical value beyond which the IFW inside the shaft would become unstable or even disappear.

Observation using high-speed camera

The behavior and flame shape of the IFW was also observed using a high-speed camera which is able to take up to 1000 fps. A normal camera cannot capture the fast whirling of flame because it took much less than 1 second for one revolution of the IFW. Moreover, a maximum of 2700 pictures can be stored for each test using high-speed camera. The flame shape observed was found to depend on gap widths.

A high-speed camera was used to take photographs for test T10. Two tests were conducted in the shaft with a 11.5 cm vertical gap width:



Figure 3. Test T10h1 at time 3.66-4.08 seconds (duration of 0.42 second for 105 frames), frame interval 0.004 second captured using a high-speed camera

- Test T10h1: 250 fps for 2700 frames with testing duration of 10.8 seconds (high-speed camera)
- Test T10h2: 60 fps for 2700 frames with testing duration of 45 seconds (normal camera).

For easy comparison of the flame shape, 105 (157) frames with test duration of $105/250 = 0.42$ second are put in one graph for T10h1, each frame of time interval (0.42/105 second) or 0.004 second. For test T10h2, test duration of $105/60 = 1.75$ seconds, with each frame of time interval of (1.75/105 second) or 0.0167 second are put in one graph.

The captured pictures for test T10h1 by 250 fps are shown in fig. 3 (3.66-4.08 seconds) with 105 frames of time interval of 0.004 second.

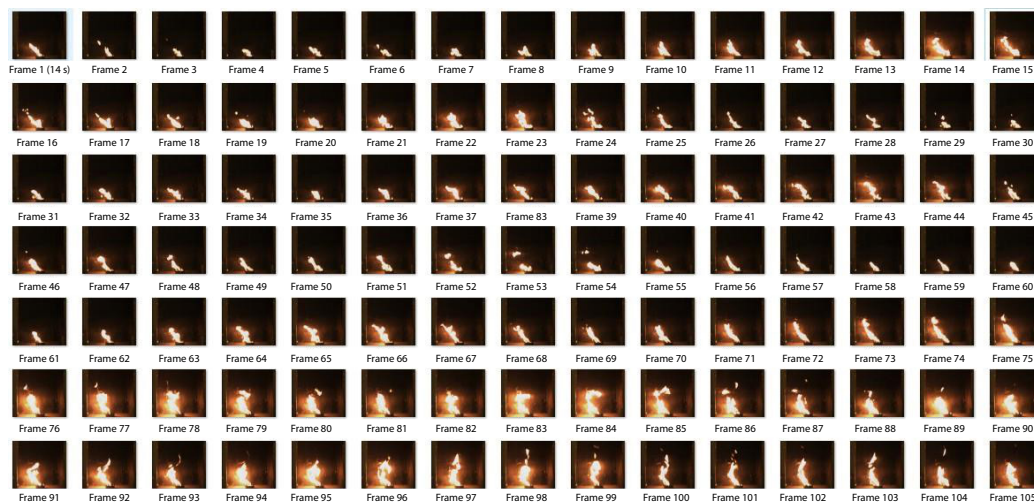


Figure 4. Test T10h2 from 14-15.75 seconds (duration of 1.75 seconds for 105 frames), frame interval 0.0167 second captured using a high-speed camera

Some photos at the transition stage (to tall flame height) and steady burning stage for test T10h2 are shown in fig. 4 (the transition from randomly revolving to flame swirling 14-15.75 seconds). The critical time periods at transition from randomly swinging flame to a fire whirl are from 23.25-25.00 seconds and from 25.00-26.75 seconds.

The following were observed from the captured pictures for the two tests:

- Test T10h1: about 2.5 rps with 90 frames for 1 revolution before generating the fire whirl.
- Test T10h2: about 2 rps with 30 frames for 1 revolution before generating the fire whirl.

The swirling rate was about 2-2.5 rps before going to the steady fire whirl stage in the shaft model with a vertical gap of 11.5 cm. The whirl rate was faster than 3 rps for steady fire whirl stage.

It is difficult or even impossible to observe the fire whirls within one revolution with a normal speed camera as shown in the aforementioned figures. However, one common point for all the IFW is that the IFW flame rotated in counterclockwise direction as the air was entrained inside the shaft through the gap which created a counter-clock-wise circulation of air inside the shaft and generated the IFW in this direction.

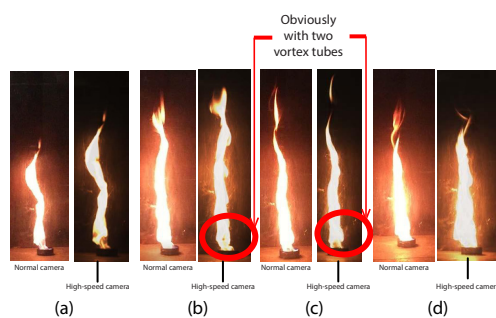


Figure 5. Pictures from a normal camera and a high-speed camera; (a) 25 seconds, (b) 50 seconds, (c) 100 seconds, and (d) 150 seconds

increasing the corner gap width to an appropriate value (with d_g/a ratio from 1/17 to 8/17) in this model, a steady fire whirl would be developed in a sequence of stages as in fig. 7. A fire plume was formed initially as in fig. 7(a), flame tilted with revolution about the central pool fire axis as in fig. 7(b), rotation (or self-spinning) with precession started about the tilted flame axis with two vortex tubes as in fig. 7(c), further tilted as in fig. 7(d) with revolution at an angle

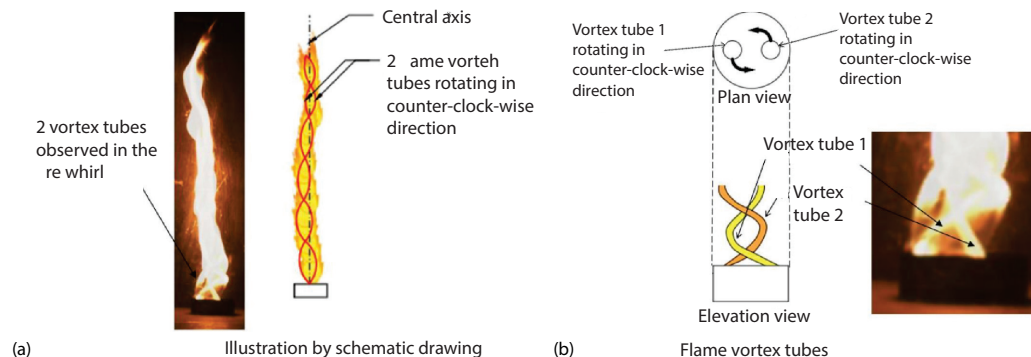


Figure 6. Flame core observed in an IFW using a high-speed camera; (a) photograph taken by a high-speed camera at 45 seconds, (b) enlarged high-speed camera photograph showing the rotating flame vortex tube

Pictures for tests at 25 seconds, 50 seconds, 100 seconds, and 150 seconds by a high-speed camera were compared with those by a normal camera in fig. 5. It is observed that there are two flame vortex tubes as in figs. 5(b) and 5(c). The observed pattern was enlarged in fig. 6 to show two vortex tubes moving over the horizontal pool surface as in fig. 6(b). A schematic of vortex lines in a thermal plume in rotation was also suggested [21].

From the previous observation, more detailed schematic diagrams than before [15, 16] can be drawn. It is observed that while

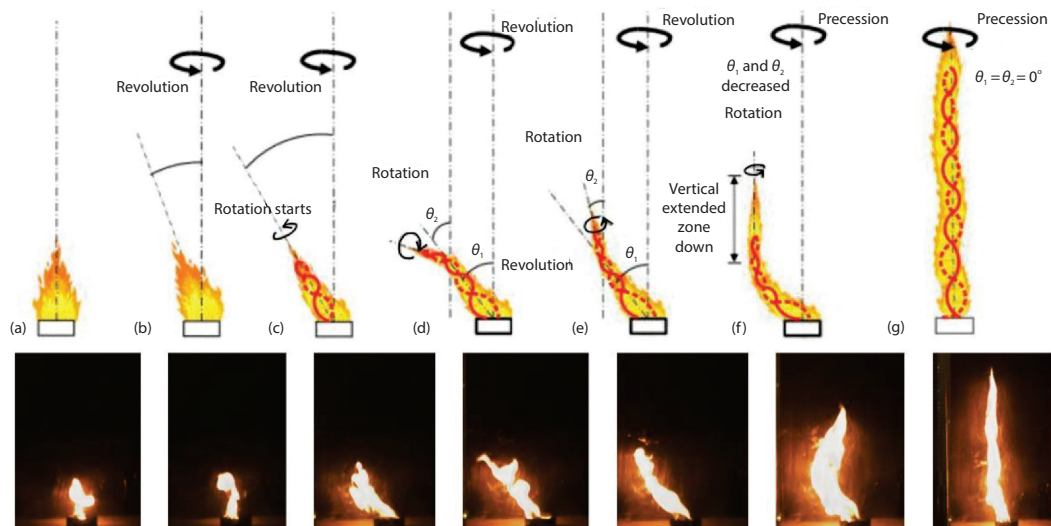


Figure 7. Stages to form an IFW from a high-speed camera; (a) free fire plume, (b) tilted flame with revolution, (c) flame tip started to rotate, (d) rotational zone formed, (e) θ_2 decreased, (f) rotational zone became vertical and moved down, and (g) an IFW formed

2 to vertical axis. Then 2 decreased as in fig. 7(e), a vertical flame part formed as in fig. 7, and eventually an IFW formed as in fig. 7(g). The two vortex tubes were observed as shown in the figure. The motion of the vortex tubes can be further explained using the theory proposed by Church *et al.* [22].

A primary anchoring zone above a pool fire was observed by Venkatesh *et al.* [23]. Using video camera of 30 fps, flame shapes of an IFW of 5 cm diameter pool fire was also observed by Chuah and Kushida [24] to have some air regions above the burning fuel surface. An air region was observed in an IFW from a 5 cm diameter methanol pool fire by Chuah *et al.* [25]. Spinning of flame base of a 3 cm diameter ethanol pool fire would give higher burning rate as reported by Kuwana *et al.* [26]. There was also an air region observed, though the flame vortex tubes could not be seen clearly.

The maximum flame heights f_{\max} [cm] and average flame height f_h [cm] are shown in tab. 1.

Empirical expression derived from experimental observation

The flame of an IFW as formed in fig. 7(g) can be taken as a fast rotating cylindrical diffusion flame. Based on this observed pattern, an axis of symmetry is formed along the vertical centerline with air entrained horizontally from all directions. An IFW is a complex 3-D flow field and the surface of the flame has a helical structure. Within an average time, the flow field of the fire whirl can be taken as axis-symmetric.

Comparing with a normal pool fire, the flame surface of an IFW is relatively stable without having large-scale eddies and low buoyancy. Centrifugal force and density gradient along the radial direction would give a stable condition as reported in an analytical study of IFW before [20]. In this long-term project [11-15] studying IFW generated by a pool fire in a vertical shaft, a high-speed camera was used to observe better swirling flow generation patterns of the fire whirl in this paper. The flame surface of the IFW is smooth without so many wrinkles due to turbulent stratification effect. Mixing and burning of fuel and air would reduce

the flame diameter of fire whirl $R(z)$ axially, then further reduce it to almost the central axis at the top part of the fire. However, the change in flame diameter is small in a fire whirl with a tall axial height. Hence, the flame diameter, $R(z)$, is assumed to be a constant, R .

The buoyant axisymmetric plume mass-flow rate \dot{m}_{plume} [kgs⁻¹] at some height, z , above the fuel source in cylindrical co-ordinates (r, θ, z) can be written in terms of the density, ρ , the axial velocity, $V_z(z, r)$, and the flame radius, R , as reported before [19]:

$$\dot{m}_{\text{plume}}(z) = \int_0^{\infty} (2\pi r) \rho V_z(z, r) dr \approx \int_0^R (2\pi r) \rho V_z(z, r) dr \quad (1)$$

The plume mass-flow increases steadily with height, since ambient air is continually entrained over the plume height. This mass consists of a mixture of combustion products and ambient air entrained into the plume, with most of the mass originating from the ambient air entrained and only a small portion originating from the combustion products. The plume mass-flow rate at the mean flame height, f_h , can be written as a sum of the burning rate, \dot{m} , and the total air entrainment rate, \dot{m}_{entr} :

$$\dot{m}_{\text{plume}}(z) \Big|_{z=f_h} = \dot{m} + \dot{m}_{\text{entr}} \approx \dot{m}_{\text{entr}} \quad (2)$$

But \dot{m}_{entr} is given:

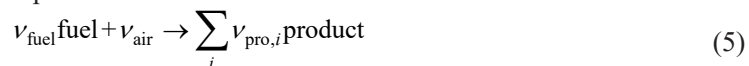
$$\dot{m}_{\text{entr}} = \int_0^{f_h} \frac{d\dot{m}_{\text{plume}}}{dz} dz \quad \text{or} \quad \dot{m}_{\text{entr}} \int_0^{f_h} \frac{d}{dz} \left[\int_0^R \rho V_z (2\pi r) dr \right] dz \quad (3)$$

The study approach is a good starting point aims at describing the correlations between the upward plume motion, air entrainment, combustion product flow and air intake from the shaft gap.

In this vertical shaft model, the rotation of buoyant flame above a gasoline pool was induced by incoming tangential air-flow from a sidewall corner gap. The total air intake rate to the flame can be expressed in terms of the air velocity at corner gap, $V_d(z)$, and the width of sidewall corner gap d_g as:

$$\dot{m}_{\text{in}} = \int_0^{f_h} d_g \rho_{\infty} V_d dz \quad (4)$$

For combustion reaction with stoichiometric coefficients ν_i , ν_g , and $\nu_{\text{pro},i}$ of the i^{th} product for the overall combustion process:



Stoichiometric eq. (5) gives the mass consumption rates for fuel and oxidizer per unit volume (\dot{m}_{fuel}^m and \dot{m}_{air}^m) related to the molecular weights M_{fuel} and M_{air} :

$$\frac{\dot{m}_{\text{fuel}}^m}{\nu_{\text{fuel}} M_{\text{fuel}}} = \frac{\dot{m}_{\text{air}}^m}{\nu_{\text{air}} M_{\text{air}}} \quad (6)$$

The stoichiometric air-fuel ratio s is defined:

$$s = \frac{\nu_{\text{air}} M_{\text{air}}}{\nu_{\text{fuel}} M_{\text{fuel}}} \quad (7)$$

Although air entering through the gap might not enter into the flame directly, circular motion will be induced to affect indoor air-flow pattern. Part of the air-flow rate coming from

this single gap would sustain combustion. A starting point of analysis is to introduce a specific proportion for this ratio. Mass burning rate of the fuel and air-flow rate entrained from the gap might not be linearly correlated. Therefore, a log-log fitting is then used for further analysis.

The mass loss rate of the fuel, \dot{m} , is assessed to relate to a power of dimensionless flame height and critical gap width $f_h^* d_g^*$ with some exponent. The power law can be justified by plotting log-log fitting.

Assuming that a constant proportion of entrained fresh air would react with fuel in flame, the burning rate \dot{m} [kgs⁻¹] can be expressed:

$$\dot{m} = \frac{\gamma \dot{m}_{in}}{s} \quad (8)$$

If distribution of the velocity $V_d(z)$ is known, then the relation between burning rate \dot{m} , width of corner gap d_g , and flame height f_h can be estimated. Several assumptions have been made and justified before while studying variation of air velocity through the gap along the radial direction, V_d , with height z by Zou *et al.* [20] with the maximum flame height reported before. The following expression was suggested in terms of a constant, K , after derivation:

$$\dot{m}_{in} = K f_h^* d_g^* \quad (9)$$

Dimensionless flame height f_h^* in terms of D , and d_g^* in terms of vertical shaft width a [m] with the gap are given:

$$f_h^* = \frac{f_h}{D} \quad (10)$$

$$d_g^* = \frac{d_g}{a} \quad (11)$$

Therefore, plotting $\ln \dot{m}_{in}$ against $\ln f_h^* d_g^*$ should give a straight line.

Three mass loss rate averages

The change of fuel mass with time was measured by placing the pool on an electronic balance with accuracy of 0.001 g. The average burning rate was estimated by three values \dot{m}_{av1} and \dot{m}_{av2} based on the burning duration t_B and fire swirling time shown in tab. 1 and fig. 8(a):

$$\dot{m}_{av1} = \frac{\text{mass of fuel lost}}{t_B} \quad (12)$$

$$\dot{m}_{av2} = \frac{\text{mass of fuel lost}}{\text{swirling time}} \quad (13)$$

From the table, $\dot{m}_{av1} = 19.6 \text{ g}/t_B$ and $\dot{m}_{av2} = 19.6 \text{ g}/t_{fw}$.

Another value \dot{m}_{av3} was also estimated based on the average of the transient mass loss rates over the swirling time with a fire whirl.

The following linear expressions are fitted in this study with correlation coefficient being 0.886 and 0.705, respectively, fig. 8(b):

$$\ln \dot{m}_{av1} = -0.152 \ln f_h^* d_g^* - 2.064 \quad (14)$$

$$\ln \dot{m}_{av2} = -150 \ln f_h^* d_g^* - 1.959 \quad (15)$$

Further, \dot{m}_{av3} based on the transient mass loss of propanol is also fitted using the following expression, the correlation coefficient being 0.44596:

$$\ln \dot{m}_{av3} = -0.372 \ln f_h^* d_g^* - 2.127 \tag{16}$$

The aforementioned correlations suggested that eq. (9) holds in estimating \dot{m} by eq. (8).

Mass loss rate fluctuated at transient stages. It is difficult to compare the flame heights and mass loss rates at any quasi-steady-state for different test scenarios. Average values of flame heights and three estimates on average mass loss rates as in previous under typical conditions including total burning duration and total whirling time.

Further, correlation of flame height of IFW with the gap width can be deduced by plotting f_d^* against d_g^* . As shown in fig. 8(c), a line is fitted for using data \dot{m}_{av1} with high value of correlation coefficient of 0.9544:

$$f_h^* d_g^* = 6.82 d_g^* + 0.458 \tag{17}$$

For using data \dot{m}_{av2} and \dot{m}_{av3} together because they are based on the same flame swirling stage, another line with correlation coefficient 0.9141 can be fitted:

$$f_h^* d_g^* = 5.14 d_g^* + 0.489 \tag{18}$$

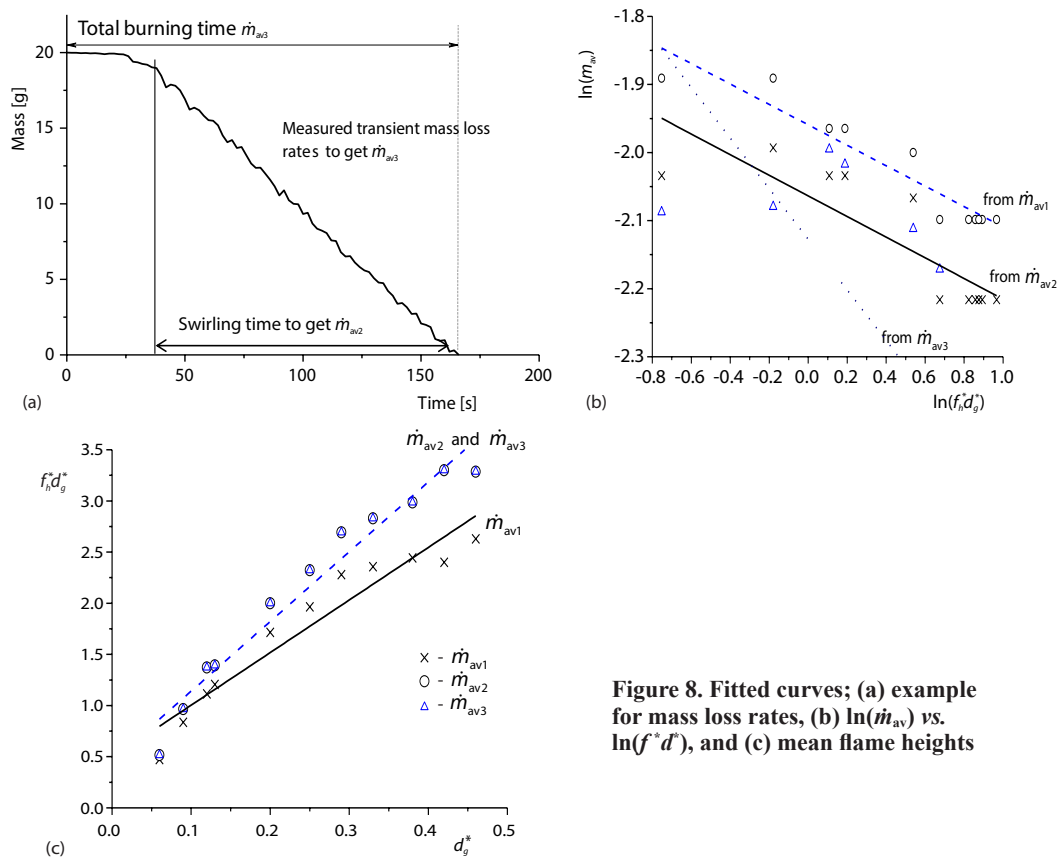


Figure 8. Fitted curves; (a) example for mass loss rates, (b) $\ln(\dot{m}_{av})$ vs. $\ln(f^* d^*)$, and (c) mean flame heights

Therefore, air-flow rate across the gap, \dot{m}_{in} , is related to d_g^* . One of the goals of this long-term research project [11-15] is to study the correlation of the flame height of an IFW with the corner gap width. A more general correlation can be derived by introducing critical gap width (ratio) and dimensionless flame height which involved the effect of the fuel pool diameter.

Conclusions

Experimental observation on earlier full-scale burning tests indicates that an IFW can be generated by a gasoline pool fire burning in a square vertical shaft model with a single sidewall corner gap with widths lying within an appropriate range. For gap widths wider or narrower than this range, the pool fire appears either as free burning or fire revolution.

By using a high-speed camera, two vortex tubes were observed now which moved around the horizontal pool fire surface. As the motion was quite fast, it was difficult to see the vortex tubes in the fire whirl before. Based on the corresponding flame swirling observed in experiments and compiled data, and an analytical study on vertical distribution of the radial velocity, a correlation of the flame height of an IFW with the corner gap width has been obtained. More experimental data for further study is needed and in depth study shall be conducted later. The results of the present study would be useful to determine fire safety provisions for vertical shafts in tall buildings where IFW might be generated.

Acknowledgment

The work described in this paper was supported by a grant from the Research Grants Council of the Hong Kong Special Administrative Region, China for the project *A study on electric and magnetic effects associated with an internal fire whirl in a vertical shaft* (Project No. PolyU15206215) with account number B-Q47D.

Nomenclature

a	– wall width, [cm]	\dot{m}_{in}	– air-flow rate across the gap, [kgs ⁻¹]
D	– diameter, [cm]	\dot{m}_{plume}	– plume mass- flow rate, [kgs ⁻¹]
d_g	– gap width, [cm]	\dot{m}_{air}^m	– mass consumption rate for oxidizer fuel per unit volume, [kgm ⁻³ s ⁻¹]
d_g^*	– critical gap width, [cm]	\dot{m}_{fuel}^m	– mass consumption rate for fuel per unit volume, [kgm ⁻³ s ⁻¹]
f_{max}	– maximum flame height, [cm]	R	– flame radius, [cm]
f_h	– average flame height, [cm]	s	– stoichiometric air-fuel ratio
f_h^*	– dimensionless flame height, [-]	t_B	– burning time, [s]
M_{air}	– molecular weight of air, [kg]	V_z	– axial velocity, [ms ⁻²]
M_{fuel}	– molecular weight of fuel, [kg]	V_d	– air velocity at corner gap, [ms ⁻²]
\dot{m}	– burning rate, [kgs ⁻¹]	z	– height, [cm]
\dot{m}_{av1}	– average mass loss rate over burning time, [gs ⁻¹]	<i>Greek symbols</i>	
\dot{m}_{av2}	– average mass loss rate over fire whirl, [gs ⁻¹]	ν_i, ν_g, ν_{prod}	– stoichiometric coefficients of the i^{th} product for the overall combustion process
\dot{m}_{av3}	– average mass loss rate by measuring transient mass, [gs ⁻¹]	ρ	– density [kgm ⁻³]
\dot{m}_{entr}	– air entrainment rate, [kgs ⁻¹]		

References

- [1] Emmons, H. W., Fundamental Problems of the Free Burning Fire, *Proceedings*, 10th International Symposium on Combustion, The Combustion Institute, Cambridge, UK, 1964, pp. 951-964
- [2] Byram, G. M., Martin, R. E., The Modelling of Fire Whirlwinds, *Forest Science*, 16 (1970), 4, pp. 386-399
- [3] Morton, B. R., The Physics of Fire Whirls, *Fire Research Abstracts and Reviews*, 12 (1970), 1, pp. 1-19
- [4] Soma, S., Saito, K., Reconstruction of Fire Whirls Using Scale Models, *Combustion and Flame*, 86 (1991), 3, pp. 269-284

- [5] Satoh, K., Yang, K. T., Measurements of Fire Whirls from a Single Flame in a Vertical Square Channel with Symmetrical Corner Gaps, *Proceedings of ASME Heat Transfer Division-1999, 1999 ASME IMECE, HTD, 364* (1999), 4, pp. 167-173
- [6] Battaglia, F., et al., Simulating Fire Whirls, *Combustion Theory and Modelling*, 4 (2000), 2, pp. 123-138
- [7] Meroney, R. N., Fires in Porous Media: Natural and Urban Canopies, in: *Flow and Transport Processes with Complex Obstructions* (Eds. Y. A. Gayev and J. C. R. Hunt), Springer, Dordrecht, 2007, Chapter 8, pp. 271-310
- [8] Klimenko, A. Y., Williams, F. A., On the Flame Length in Firewhirls with Strong Vorticity, *Combustion and Flame*, 160 (2013), 2, pp. 335-339
- [9] Lei, J., Liu, N., Flame Precession of Fire Whirls: A Further Experimental Study, *Fire Safety Journal*, 79 (2016), Jan., pp. 1-9
- [10] Hayashi, Y., et al., Influence of Vortex Parameters on the Flame Height of a Weak Fire Whirl via Heat Feedback Mechanism, *Journal of Chemical Engineering of Japan*, 46 (2013), 10, pp. 689-694
- [11] Chow, W. K., Han, S. S., Experimental Investigation on Onsetting Internal Fire Whirls in a Vertical Shaft, *Journal of Fire Sciences*, 27 (2009), 6, pp. 529-543
- [12] Zou, G. W., et al., Numerical Studies on Fire Whirls in a Vertical Shaft, *Proceedings, 2009 US-EU-China Thermophysics Conference-Renewable Energy (UECTC-RE '09)*, Beijing, China, 2009
- [13] Chow, W. K., et al., Internal Fire Whirls in a Vertical Shaft, *Journal of Fire Sciences*, 29 (2011), 1, pp. 71-92
- [14] Chow, W. K., A Study on Relationship between Burning Rate and Flame Height of Internal Fire Whirls in a Vertical Shaft Model, *Journal of Fire Sciences*, 32 (2014), 1, pp. 72-83
- [15] Zou, G. W., Chow, W. K., Generation of an Internal Fire Whirl in an Open Roof Vertical Shaft Model with a Single Corner Gap, *Journal of Fire Sciences*, 33 (2015), 3, pp. 183-201
- [16] Chow, W. K., Performance-Based Approach to Determining Fire Safety Provisions for Buildings in the Asia-Oceania Regions, *Building and Environment*, 91 (2015), Sept., pp. 127-137
- [17] Chow, W. K., Numerical Studies of Air-Flows Induced by Mechanical Ventilation and Air-Conditioning (MVAC) Systems, *Applied Energy*, 68 (2001), 2, pp. 135-159
- [18] Chow, W. K., Chan, K. T., Parameterization Study of the Overall Thermal-Transfer Value Equation for Buildings, *Applied Energy*, 50 (1995), 3, pp. 247-268
- [19] Williams, F. A., Scaling Fire Whirls, Keynote Lecture, *Proceedings, 8th International Symposium on Scale Modelling (ISSM-8)*, Portland, Ore., USA, 2017
- [20] Zou, G. W., et al., A Study of Correlation between Flame Height and Gap Width of an Internal Fire Whirl in a Vertical Shaft with a Single Corner Gap, *Indoor and Built Environment*, 28 (2017), 1, pp. 34-45
- [21] De Ris, J., Scale Modelling of Fires, Keynote Lecture, *Proceedings, 8th International Symposium on Scale Modelling (ISSM-8)*, Portland, Ore., USA, 2017
- [22] Church, C. R. et al., Intense Atmospheric Vortices Associated with a 1000 MW Fire, *Bulletin of the American Meteorological Society*, 61 (1980), 7, pp. 682-694
- [23] Venkatesh, S., et al., Flame Base Structure of Small-Scale Pool Fires, *Proceedings, 26th International Symposium on Combustion*, Pittsburgh, Penn., USA, 1996, pp. 1437-1443
- [24] Chuah, K. H., Kushida, G., The Prediction of Flame Heights and Flame Shapes of Small Fire Whirls, *Proceedings of Combustion Institute*, 31 (2007), 2, pp. 2599-2606
- [25] Chuah, K. H. et al., Modelling Fire Whirl Generated over a 5-cm-Diameter Methanol Pool Fire, *Combustion and Flame*, 156 (2009), 9, pp. 1828-1833
- [26] Kuwana, K., et al., The Burning Rate's Effect on the Flame Length of Weak Fire Whirls, *Proceedings of Combustion Institute*, 33 (2011), 2, pp. 2425-2432